



Di Laora, R., Galasso, C., Mylonakis, G., & Cosenza, E. (2020). A simple method for N-M interaction diagrams of circular reinforced concrete cross-sections. *Structural Concrete*, 21(1), 48-55.
<https://doi.org/10.1002/suco.201900139>

Peer reviewed version

Link to published version (if available):
[10.1002/suco.201900139](https://doi.org/10.1002/suco.201900139)

[Link to publication record in Explore Bristol Research](#)
PDF-document

This is the author accepted manuscript (AAM). The final published version (version of record) is available online via Wiley at <https://onlinelibrary.wiley.com/doi/full/10.1002/suco.201900139> . Please refer to any applicable terms of use of the publisher.

University of Bristol - Explore Bristol Research

General rights

This document is made available in accordance with publisher policies. Please cite only the published version using the reference above. Full terms of use are available:
<http://www.bristol.ac.uk/red/research-policy/pure/user-guides/ebr-terms/>

A simple method for N-M interaction diagrams of circular reinforced concrete cross-sections

Raffaele Di Laora^{1*}, Carmine Galasso², George Mylonakis³, and Edoardo Cosenza⁴

¹Assistant Professor, Department of Engineering, Università degli Studi della Campania “Luigi Vanvitelli”, Aversa (CE), Italy

²Associate Professor, Department of Civil, Environmental & Geomatic Engineering, University College London, UK

³Professor, Department of Civil Engineering, University of Bristol, UK; Professor, University of Patras, Greece; Adjunct Professor, University of California, Los Angeles, USA

⁴Professor, Dipartimento di Strutture per l’Ingegneria e l’Architettura, Università degli Studi di Napoli “Federico II”, Naples, Italy

ABSTRACT

A novel closed-form expression is derived for the ultimate capacity interaction diagram (i.e., axial compression-bending moment resistance in N-M space) of reinforced concrete (RC) columns with circular cross-section. To this aim, the longitudinal rebar arrangement is replaced with a thin steel ring equivalent to the total steel area; moreover, according to modern design approaches, simplified stress-strain relationships for concrete and reinforcing steel are used. Illustrative applications demonstrate that the ultimate capacity computed by the proposed analytical approach agrees well with the results obtained by rigorous methods based on consolidated numerical algorithms. The new solution allows rapid, accurate assessments of cross-section capacity by means of hand calculations; this is especially useful at the conceptual design stage of various structural and geotechnical systems. The solution can be extended to more general configurations, such as multiple steel rings and composite

concrete-steel sections.

Keywords: reinforced concrete, circular cross-section, interaction diagram, simplified formulation, analytical solution.

INTRODUCTION

Reinforced concrete (RC) structural members with circular cross-section are widely used in structural and geotechnical engineering applications. Typical examples include columns in moment-resisting frames, foundation piles, and contiguous pile walls. The widespread use of circular cross-sections in structural members is mainly due to their simplicity of construction as well as to their identical stiffness and strength characteristics in all horizontal directions. However, while the design of rectangular RC cross sections may be easily performed, even by hand calculations under some simplifying assumptions, for circular cross-sections, the analysis is more complex. In absence of analytical closed-form solutions, the assessment of axial compression-bending moment resistance (M-N) interaction domains can be performed only numerically.

Research on the topic includes integration methods for rectangular and circular RC cross-sections based on analytical and numerical algorithms (e.g., [Bonet et al., 2006](#); [Elevard, 1997](#); [Brondum Nielsen, 1988](#); [Davalath et al., 1988](#)). For instance, Bonet et al. (2006) presented a comparative study of different integration methods (both analytical and numerical) of stresses in circular and rectangular RC cross-sections subjected to axial loads and biaxial bending. The constitutive equation used for concrete is a parabola-rectangle from Eurocode 2 ([CEN, 2004](#)). The comparison is performed in terms of accuracy and computational speed of each investigated method. Similarly, [Davalath et al. \(1988\)](#) developed a numerical procedure along with a computer code for the analyses design of RC circular cross-sections subjected to axial loads (compression or tension) and bending moments.

1 [Barros et al. \(2004\)](#) derived a closed-form solution for the optimal design of RC cross-
2 sections, but only for the rectangular shape. This method is valid for ultimate axial and
3 (uniaxial) bending loading; it relies on the use of a parabola-rectangle diagram for the
4 concrete in compression. Furthermore, [Tumo et al. \(2009\)](#) have presented an analytical
5 approach for quantifying the contribution of transverse reinforcement to the shear resistance
6 of RC structural members of solid and hollow circular cross-section. Recently, [Trentadue et](#)
7 [al. \(2016\)](#) proposed closed-form approximations of the M-N interaction domains for RC
8 columns and concrete-filled steel tubes with circular cross-section. A single closed-form
9 expression is provided for both cases; however, one parameter (which is function of the
10 mechanical ratio of the reinforcing steel) of the proposed approach has still to be calibrated
11 by means of a numerical optimization procedure.

12 This short paper introduces a fully analytical, code-compatible procedure for the ultimate
13 analysis of RC circular cross-sections subjected to axial compression and bending. The study
14 constitutes an improvement over the method proposed in [Cosenza et al. \(2011\)](#). As in the
15 previous study, the equations are developed by assuming the reinforcement steel area as
16 lumped into an equivalent steel ring completely yielded, whereas the stress-block diagram is
17 assumed for concrete. In addition, design yield stress of steel is properly modified to obtain
18 more accurate results. Moreover, an analytical approximation is introduced to derive a
19 closed-form solution for the computation of M-N domains without iterations and/or
20 numerical work.

21 The rest of this paper is organized as follows. A review of code-based assumptions and
22 procedures for the assessment of the ultimate flexural capacity of RC cross-section is
23 presented first. The proposed analytical method is then described, introducing a simplified
24 approach for the derivation of M-N domains. This is followed by a validation exercise for the
25 proposed method through a series of illustrative examples.

CODE-BASED ASSESSMENT OF ULTIMATE FLEXURAL CAPACITY FOR RC CROSS-SECTIONS

Eurocode 2 (or EC2; CEN, 2004, Sec. 6.1) provides principles and rules for the assessment of the ultimate flexural capacity of RC members, with or without axial force. To this end, the following simplifying assumptions are made:

1. Plane cross-sections remain plane upon deformation, up to failure;
2. Strain in bonded reinforcement (whether in tension or in compression), is identical to that in the surrounding concrete (i.e., perfect bonding exists between steel and concrete);
3. The tensile strength of the concrete is neglected;
4. Compressive stresses in concrete are derived according to pertinent idealized design stress/strain relationships (EC2, Sec. 3.1.7);
5. Stresses in reinforcing bars are derived from corresponding design curves (EC2, Sec. 3.2.7);
6. Design strengths for concrete and steel are defined as $f_{cd} = \alpha_{cc} \frac{f_{ck}}{\gamma_c}$ and $f_{yd} = \frac{f_{yk}}{\gamma_s}$, respectively (EC2, Secs. 3.1.6, 3.2.7), where α_{cc} is a coefficient taking into account of long term effects on compressive strength and of unfavorable effect resulting from the way the load is applied¹, f_{ck} is the specified (i.e., characteristic, 5%) compressive strength of concrete (cylinder strength) and f_{yk} is the specified yield stress of steel, γ_c and γ_s are material safety factor according to Eurocode-like Load and Resistance Factor Design (LRDF);
7. Material safety factors are $\gamma_c = 1.5$ for concrete and $\gamma_s = 1.15$ for steel (EC2, Sec. 2.4.2.4).

¹ According to EC2, the value of α_{cc} for use in a Country should lie between 0.8 and 1.0 and the recommended values is 1.

It is worth noting that all the above assumptions also hold in the case of [ACI 318-14 \(2014\)](#). The main difference is that the Eurocode-based approach to LFRD consists of reducing the material ultimate strength values using their conservative percentiles (i.e., characteristic values divided by material safety factors) as design values rather than applying safety factors directly to the sectional strength (as in the ACI 318-14 - see [Iervolino and Galasso \(2012\)](#) for an extensive discussion on the topic). On the other hand, the specified compressive strength of concrete and the specified yield strength for nonprestressed reinforcement in ACI 318-14 are directly used to compute the nominal flexural strength of a cross-section and this is further reduced by a strength reduction factor in ACI 318-14 (*Chapter 21*), ranging from 0.65 to 0.90 for moment, axial force, or combined moment and axial force.

According to points 4) and 5), a rigorous assessment of the ultimate flexural capacity may be performed assuming a parabolic-rectangular relationship between the stress and corresponding strain in the concrete in compression, whereas the steel may be idealized as an elastoplastic-material (Fig. 1a). Such an analysis requires the use of integration procedures and is thereby performed via computer codes—such as Biaxial software ([Di Ludovico et al., 2010](#)). As a simpler alternative for the analysis and design of circular cross-sections at the Ultimate Limit State (ULS), simplified stress-strain relationships may be utilized. For instance, similarly to ACI 318-14, the stress distribution in the concrete may be assumed as a rectangular stress block extended up to a depth, y , smaller than of the actual neutral axis depth, x , and a magnitude, f'_{cd} , equal to some fraction of the concrete compressive design strength (generally, $y = 0.8x$ and $f'_{cd} = f_{cd}$ are assumed). This procedure means, in terms of constitutive models of the materials, that concrete behaves as a perfectly plastic material after reaching a specific threshold value of compressive strain, whereas below such a strain value it offers no resistance (Fig. 1b). In the framework of simplified methods, an elastic-plastic stress-strain diagram for reinforcing steel, with a horizontal top branch without a strain limit,

is recommended. This latter assumption is well justified by experimental results (see for example Galasso et al. 2014). Based on this assumption, the failure of the section always occurs due to concrete crushing, i.e., when the maximum concrete strain is equal to an ultimate strain value ε_{cu} (maximum concrete compressive strain) or to a second value ε_{c2} when the section is all under compression. These deformation characteristics for concrete depend on material strength; see for example Table 3.1 in EC2.

Due to these simplified assumptions, the computation of the flexural capacity is quite straightforward by solving the equilibrium equations, yet some iterations are necessary to calculate the position of the neutral axis. A step-by-step presentation of the procedure is provided in Cosenza et al., (2011).

PROPOSED METHOD

A rigorous analysis of circular cross-sections should be performed considering the actual location of the reinforcement longitudinal bars. Such a condition does not allow a simple analytical expression to be derived for the ultimate bending moment capacity. An approximate formulation is possible by means of some straightforward idealizations specifically (Fig. 1c):

1. The actual longitudinal rebar arrangement is replaced by a thin steel ring with equivalent total area A_s ;
2. The actual distribution of concrete stress is replaced by a rectangular diagram with an “effective strength” $f'_{cd} = 0.9f_{cd}$;
3. The steel is considered to be at a yielding state, both in compression and tension, contributing an “effective stress” $f'_{yd} = 0.95f_{yd}$.

It is worth noting that these assumptions are equivalent to assuming a perfectly plastic behavior for both steel and concrete, where the threshold strain value (1) separating

compression and tension for steel and (2) below which concrete offers no strength has a given, positive value. Hence, for the assessment of the ultimate flexural capacity, regardless of the actual strain profile, materials may be assumed to behave as rigid-plastic, and the resulting (fictitious) neutral axis depth will coincide with the extension of the compressive zone. Owing to these hypotheses, the condition of equilibrium between all the internal and external forces applied to the cross-section may be written as:

$$\frac{R^2}{2}(2\theta - \sin 2\theta)f'_{cd} + \left(\frac{\theta}{\pi}\right)A_s f'_{yd} - \left(\frac{\pi - \theta}{\pi}\right)A_s f'_{yd} = N_{Ed} \quad (1)$$

where N_{Ed} is the applied axial force and θ is the angle defining the extension of compression zone (Fig. 2), ideally varying from 0 (no compression) to π (the section is entirely compressed). In Eq. (1), $\left(\frac{\theta}{\pi}\right)A_s$ and $\left(\frac{\pi - \theta}{\pi}\right)A_s$ are the cross-sectional areas of longitudinal reinforcement in compression and tension respectively.

Multiplying each term in Eq. (1) by $\frac{2}{R^2 f'_{cd}}$, Eq. (1) may be reformulated as:

$$(2\theta - \sin 2\theta) + 2\omega'\theta - 2\omega'(\pi - \theta) = 2\pi\nu' \quad (2)$$

where $\omega' = \frac{A_s}{\pi R^2} \frac{f'_{yd}}{f'_{cd}}$ and $\nu' = \frac{N_{Ed}}{\pi R^2} \frac{1}{f'_{cd}}$ are the mechanical steel ratio and the design axial force normalized to the total cross-sectional concrete area of the member (the prime symbol “ ’ ” indicates that quantities are normalized by effective values of design strength – see point 2 and 3 above).

Due to the transcendental nature of Eq. (2), the value of the angle θ may be found only iteratively (e.g., using the Newton's method). Nevertheless, an approximate solution for θ is

1 possible by substituting the term $\sin 2\theta$ in Eq. (2) with the parabola $\frac{16}{\pi^2}\theta\left(\frac{\pi}{2}-\theta\right)$ (for

2 $\theta \leq \frac{\pi}{2}$). Consequently, Eq. (2) reduces to the second-order algebraic equation:

$$3 \quad \frac{16}{\pi^2}\theta^2 + 2\left(1 + 2\omega' - \frac{4}{\pi}\right)\theta - 2\pi(\omega' + \nu') = 0 \quad (3)$$

4 which admits the positive solution:

$$5 \quad \theta = \left(\frac{\pi}{4}\right)^2 \left[\left(1 + 2\pi - \frac{4}{\pi}\right) + \sqrt{\left(1 + 2\pi - \frac{4}{\pi}\right)^2 + \frac{32}{\pi}(\omega' + \nu')} \right] \quad (4)$$

6 A comparison between the exact values of θ obtained from Eq. (2) (exact relationship among

7 θ , ν' and ω' may be found by fixing the values of θ and ν' , and calculating ω' , or fixing θ and

8 ω' and calculating ν') and the correspondent estimates by means of Eq. (4) is offered in Fig. 3,

9 as a function of dimensionless axial force ν' and reinforcement ratio ω' . Clearly, approximate

10 estimates and exact values are almost coincident. Note that the simplified expression for θ is

11 valid for $\nu' \leq 0.5$, i.e., $\theta \leq \frac{\pi}{2}$. Nevertheless, as the function $\theta(\nu')$ presents a symmetry point

12 around $(0.5, \pi/2)$, for $\nu' > 0.5$ the value of θ may be easily derived by symmetry

13 considerations.

14 Once evaluated θ , the design flexural capacity M_{Rd} is equal to the sum of the design flexural

15 resistance due to concrete, $M_{Rd,c}$, and the design flexural resistance due to steel, $M_{Rd,s}$. By

16 employing the quantities in Fig. 2, it is straightforward to show that²:

$$17 \quad M_{Rd} = M_{Rd,c} + M_{Rd,s} = \frac{2}{3}R^3 \sin^3 \theta f'_{cd} + \frac{2}{\pi}(R - c) A_s \sin \theta f'_{yd} \quad (5)$$

² Note that due to a clerical error, in the original work by Cosenza et al. (2011) the equation is reported with a wrong coefficient of 4/3 instead of 2/3.

1 where c is the concrete cover of cross-section; multiplying each term by $\frac{1}{2\pi R^3 f'_{cd}}$, Eq. (5)

2 may be rewritten as:

$$3 \quad \mu_{Rd} = \frac{1}{3} \frac{1}{\pi} \sin^3 \theta + \frac{\omega'}{\pi} \left(1 - \frac{c}{R} \right) \sin \theta \quad (6)$$

4 where $\mu_{Rd} = \frac{M_{Rd}}{2\pi R^3 f'_{cd}}$ is the dimensionless bending capacity of the cross-section. In this way,

5 the ultimate flexural capacity is expressed in general form as a function of the relevant

6 dimensionless parameters ω , ν and $\frac{c}{R}$.

7

8 **M-N INTERACTION DOMAINS**

9 The proposed method also allows a simple computation of the interaction domains in an

10 analytical way, by simply varying the axial force and, thereby, retrieving the value of the

11 corresponding ultimate moment capacity by means of Eq. (5) or (6). In addition, the

12 simplified assumptions adopted offer insight in the section layout at failure for some peculiar

13 situations corresponding to specific points in the domain. A sketch of a typical $M - N$ (or, in

14 dimensionless form, $\mu' - \nu'$) domain is reported in Fig. 4. Five (5) key points can be

15 identified.

16 - *Point A*. This corresponds to the extreme traction load the section can carry. In this

17 situation, no bending is allowed and the whole tensile force is carried by the steel, due

18 to the inherent assumption of no tensile strength offered by the concrete. The axial load

19 is thereby equal to the area of the steel A_s multiplied by its design strength f'_{yd} . In

20 dimensionless terms, it is immediate to derive that $\nu' = -\omega'$.

21 - *Point B*. This is the point symmetric to point A, and corresponds to pure compression.

22 Both concrete and steel mobilize their strength in any point of the section. The

corresponding axial force is given by the sum of the steel capacity $f'_{yd}A_s$ and the concrete capacity $f'_{cd} \pi R^2$. In dimensionless terms, $\nu' = 1 + \omega'$.

- *Point C*. This point is representative of pure bending. In such conditions, total compression force associated to both concrete and steel must equal the tensile steel force. This means that the depth of compression zone y_c is less than R . It is straightforward to derive that y_c is an increasing function of the amount of reinforcement ω , and tends to R when reinforcement increases up to infinity, as in the latter case concrete would give a negligible contribution compared to steel. A simplified expression for the moment capacity under pure bending is presented in [Cosenza et al. \(2011\)](#).

- *Point E*. This point corresponds to a failure condition with the same ultimate moment as in *Point C* and an associated compressive force. This means that the increase in axial force due to concrete and steel must not produce any bending moment and, therefore, the depth of compression zone is equal to $(2R - y_c)$. The same result may be obtained by considering that *Point E* is the one symmetrical to *Point C*. The axial force is equal to the ultimate compressive load of an un-reinforced section ($\nu' = 1$). The presence of the steel is therefore responsible for the finite moment capacity under normal load.

- *Point D*. This point is associated with the maximum bending capacity of the section, occurring under a dimensionless axial force $\nu' = 0.5$. It is evident that the stress-block diagram is extended up to a half cross-section, since any increase or decrease of the compression zone would lead to a decrease in the bending moment capacity.

VALIDATION OF THE PROPOSED METHOD

Figure 5 reports a comparison between the results obtained through the proposed approach and a rigorous solution in the realm of the aforementioned assumptions 1-7. Eurocode is used

as the reference code in this illustrative application; however, similar findings can be obtained by using the ACI 318-14 design framework. Results, expressed through dimensionless pairs $\nu' : \mu'$, refer to a circular cross-section having a diameter of 50 cm and a concrete cover of 5 cm. Reinforcement is represented by 10, 20, 30 and 40 bars with a diameter $\phi = 16\text{mm}$, corresponding to reinforcement ratios ρ approximately equal to 1, 2, 3 and 4% (consistent with detailing rules for local ductility of RC columns in seismic areas). Concrete and steel have design strengths $f_{cd} = 14.2\text{ MPa}$ ($\varepsilon_{cu} = 0.35\%$) and $f_{yd} = 391\text{ MPa}$, respectively (corresponding to $f_{ck} = 25\text{ MPa}$ and $f_{yk} = 450\text{ MPa}$, the latter being the recommended value in Italy). It is noted, by inspecting Figure 5, that the proposed method matches very closely the rigorous results obtained by means of freeware Biaxial (available from the website of the Italian Network of Earthquake Engineering University Labs, or ReLUIS: http://www.reluis.it/index_eng.html). The discrepancies from the rigorous analysis are of the order of 1% for ν' values relevant to earthquake engineering applications (e.g., $\nu < 0.55$, $\nu' < 0.61$), whereas the method underestimates by 5% and 10% the extreme values corresponding to an exclusively axial force. This is due to the simplifying assumption of reducing design strengths employed in the proposed method. Numerical values, corresponding to ν' ratios ranging from 0 to 0.5, are also reported in Table 1 together with other formulations. In the table, M_{rd1} is the most rigorous ultimate flexural capacity value of cross-section computed by the Biaxial software; M_{rd2} represents the same value but computed using the simplified stress-block diagram for concrete under compression and assuming the effective strength of concrete reduced by 10% according to EC2. (To this aim, an *ad hoc* MATHWORKS-MATLAB® script was developed by the authors). Finally, M_{rd3} is evaluated according to Cosenza et al. (2011), whereas M_{rd4} is the ultimate flexural capacity value of cross-section computed using the proposed method. The mean absolute error of the proposed approach is 1.43%, offering better performance in predicting the flexural capacity over that

provided by both the stress-block analysis (2.61%) and the Cosenza et al. (2011) method (3.54%). Note that the error provided by the proposed method is lower than the one by the Trentadue et al. (2016) approach, which claim report an average discrepancy of 3.2% versus numerical solutions.

CONCLUSIONS

The choice of a circular cross-section for structural members is popular in both geotechnical and structural design, due to simplicity of construction and equal strength under horizontal loading in all directions. Contrary to rectangular sections, no closed-form solutions are available to evaluate flexural capacity under a specified axial load. This paper aimed at providing a simple, approximate closed-form analytical solution in M-N space which could facilitate routine calculations. Comparison with rigorous numerical analyses indicates an excellent performance of the proposed approach (maximum discrepancies of less than 5%, typically less than 1%), outperforms existing simplified formulations, the latter being more complicated and involving iterative, or even numerical procedures.

REFERENCES

- American Concrete Institute (ACI) Committee 318, ACI 318-2014: Building Code Requirements for Structural Concrete and Commentary 2014.
- Barros H, Figueiras J. Reinforced concrete-design tables and abacus for the design of sections: moment and axial load with EC2. In: FEUP edições. 2010.
- Barros MHFM, Barros AFM, Ferreira CA. Closed form solution of optimal design of rectangular reinforced concrete sections. Engineering Computations 2004; 21(7):761-776.

1 Bonet JL, Barros MHFM, Romero ML. Comparative study of analytical and numerical
2 algorithms for designing reinforced concrete section under biaxial bending. *Computers &*
3 *Structures* 2006; 8:31-32.

4 Brøndum Nielsen T. Ultimate Flexure Capacity of Circular and Annular Cracked Concrete
5 Sections. *ACI Structural Journal* 1988; 85(4):437-441.

6 CEN, European Committee for Standardisation. Eurocode 2: Design of concrete structures.
7 Part 1-1: General rules and rules for buildings; 2004

8 Cosenza E, Galasso C, Maddaloni G. A simplified method for flexural capacity assessment of
9 circular RC cross sections. *Engineering Structures* 2011; 33(3):942–946.

10 CS.LL.PP. DM 14 Gennaio, Norme tecniche per le costruzioni. *Gazzetta Ufficiale della*
11 *Repubblica Italiana* 29; 2008 (in Italian).

12 Davalath GSR, Madugula MKS. Analysis/Design of Reinforced Concrete Circular Cross-
13 Sections. *ACI Structural Journal* 1988; 85(6):617-623.

14 Di Ludovico M, Lignola GP, Prota A, Cosenza E. Nonlinear Analysis of Cross-Sections
15 under Axial Load and Biaxial Bending. *ACI Structural Journal* 2010; 107(4):390-399.

16 Elevard NJ. Axial Load-Moment Interaction for Cross-Sections Having Longitudinal
17 Reinforcement Arranged in a Circle. *ACI Structural Journal* 1997; 94(6):695-699.

18 Galasso C, Maddaloni G, Cosenza E. Uncertainty analysis of flexural overstrength for new
19 designed RC beams, *ASCE Journal of Structural Engineering* 2014; 140(7).

20 Iervolino I, Galasso C. Comparative assessment of load-resistance factor design for FRP-
21 reinforced cross sections, *Construction and Building Materials* 2012; 34:151-161.

22 Trentadue F, Quaranta G, Marano GC. Closed-form approximations of interaction diagrams
23 for assessment and design of reinforced concrete columns and concrete-filled steel tubes
24 with circular cross-section. *Engineering Structures* 2016; 127:594–601.

Turmo J, Ramos G, Aparicio AC. Shear Truss Analogy for Concrete Members of Solid and
Hollow Circular Cross-Section. Engineering Structures 2009; 31(2):455-465.

Table1. Comparison of results obtained by the proposed formula (M_{Rd4}) and other formulations from the literature, including the most rigorous numerical solution using *Biaxial* (M_{Rd1}).

ν	ρ	M_{Rd1}	M_{Rd2}	M_{Rd3}	M_{Rd4}	$\frac{M_{Rd2} - M_{Rd1}}{M_{Rd1}}$	$\frac{M_{Rd3} - M_{Rd1}}{M_{Rd1}}$	$\frac{M_{Rd4} - M_{Rd1}}{M_{Rd1}}$
[-]	[%]	[kNm]	[kNm]	[kNm]	[kNm]	[%]	[%]	[%]
0	1	143.7	141.4	143.6	137.1	-1.60	-0.07	-4.59
	2	258.4	256.2	264.8	253.1	-0.85	2.48	-2.05
	3	365.7	361.2	377.9	361.2	-1.23	3.34	-1.23
	4	467.5	462.2	486.8	465.1	-1.13	4.13	-0.51
0.1	1	175.9	170.4	176.9	174.3	-3.13	0.57	-0.91
	2	283.6	277.3	290.2	281.6	-2.22	2.33	-0.71
	3	385.4	378.7	398.4	384.3	-1.74	3.37	-0.29
	4	483.9	475.7	504.0	484.6	-1.69	4.15	0.14
0.2	1	204.3	196.4	202.4	201.8	-3.87	-0.93	-1.22
	2	303.4	294.2	309.5	302.6	-3.03	2.01	-0.26
	3	399.2	390.0	414.0	401.4	-2.30	3.71	0.55
	4	494.6	484.7	517.1	499.0	-2.00	4.55	0.89
0.3	1	220.7	209.5	220.0	220.3	-5.07	-0.32	-0.18
	2	315.3	304.3	323.0	317.0	-3.49	2.44	0.54
	3	407.6	396.7	424.9	413.2	-2.67	4.24	1.37
	4	500.5	489.6	526.3	509.0	-2.18	5.15	1.70
0.4	1	228.0	217.8	229.9	227.3	-4.47	0.83	-0.31
	2	317.9	307.4	330.7	322.5	-3.30	4.03	1.45
	3	409.3	398.6	431.3	417.8	-2.61	5.38	2.08
	4	500.5	489.7	531.8	512.9	-2.16	6.25	2.48
0.5	1	224.7	215.2	233.0	227.3	-4.23	3.69	1.16
	2	314.4	304.6	333.2	322.6	-3.12	5.98	2.61
	3	404.4	394.5	433.3	417.8	-2.45	7.15	3.31
	4	494.6	484.6	533.5	512.9	-2.02	7.86	3.70

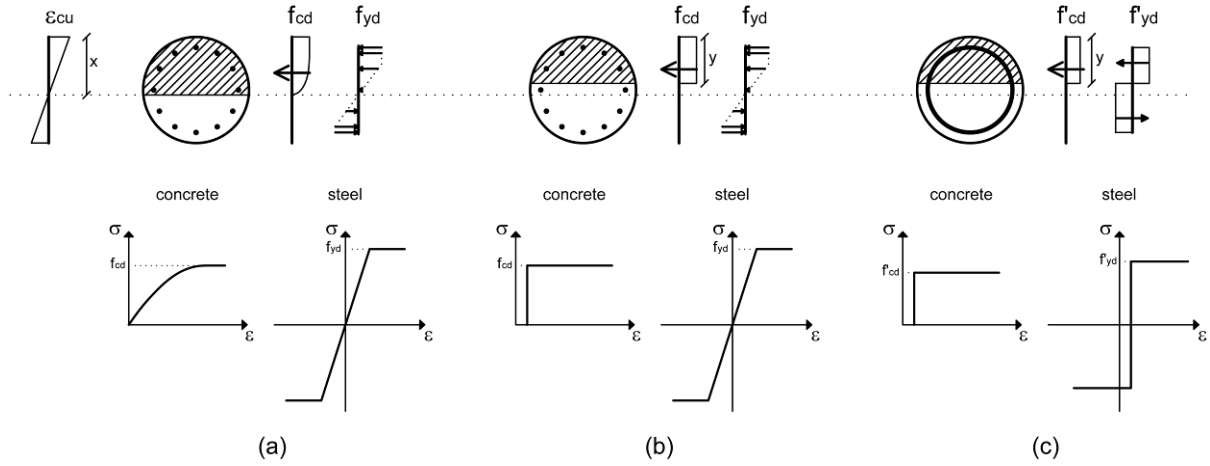


Fig. 1 Constitutive behavior of materials and mobilized strength in different analysis methods for assessment of flexural capacity of circular RC cross-sections.

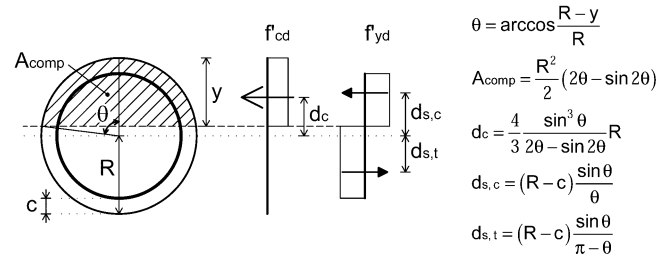


Fig. 2 Stress distribution and formulae for the proposed method.

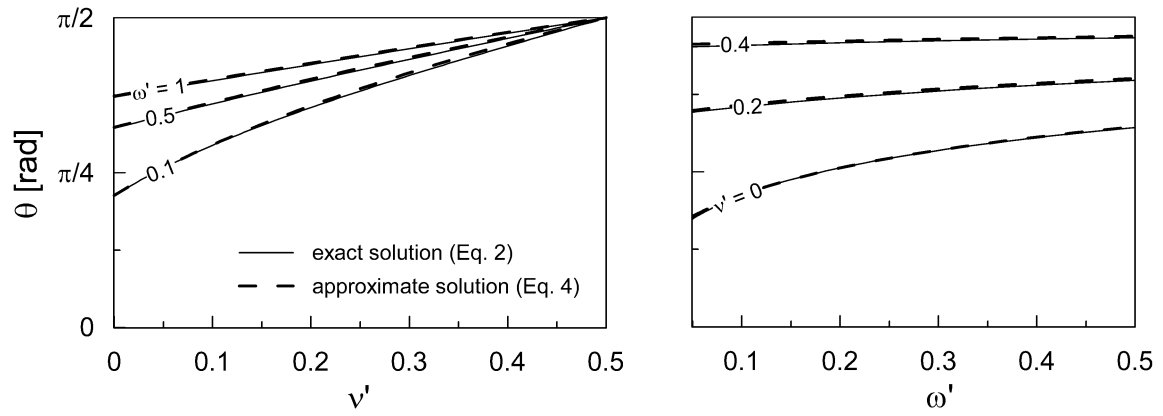


Fig. 3. Comparison between exact and approximate values of θ , as function of dimensionless axial force v' (left) and mechanical reinforcement ratio ω' (right).

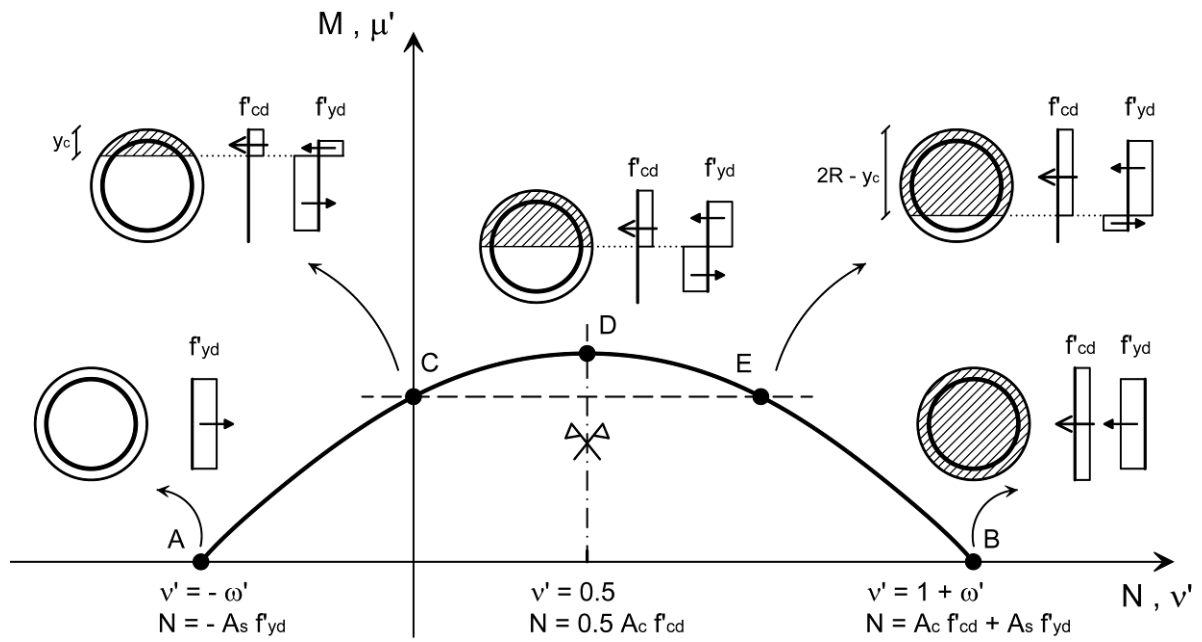


Fig. 4. N - M and v' - μ' domain by proposed method.

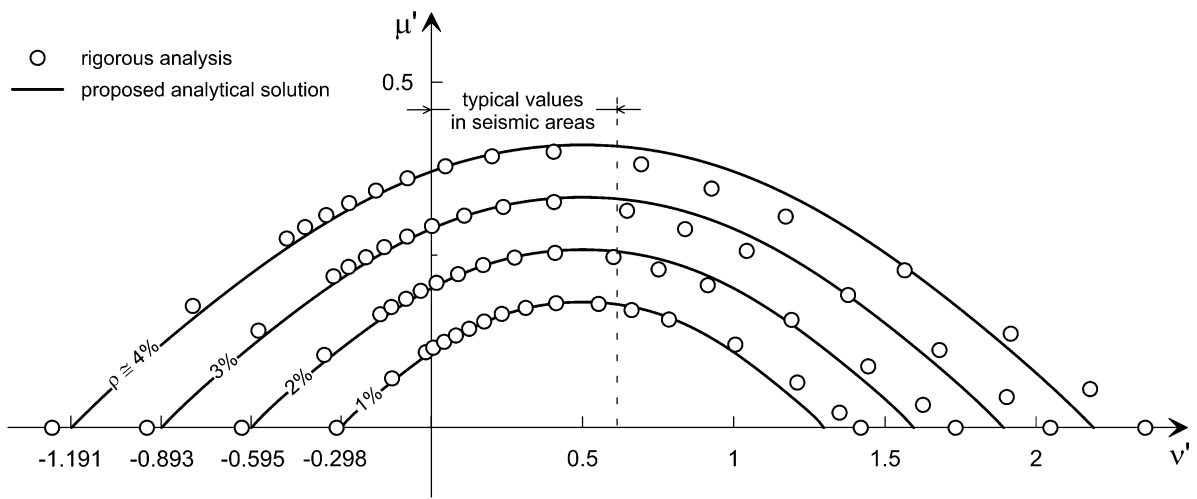


Fig. 5. Comparison between results from proposed method and other procedures.